Co-registration method for photoacoustic imaging and laser speckle imaging

Yuan Gao (高 远)[1], Yong Deng (邓 勇)[1,2,3*], Xiliang Tong (童锡良)[1], Hui Wang (王 慧)[2,3], Zilin Deng (邓子林)[2,3], Xiaoquan Yang (杨孝全)[2,3], Yanyan Liu (刘炎炎)[2,3], Hui Gong (龚 辉)[2,3], and Qingming Luo (骆清铭)[1,2,3]

[1] *College of Optoelectronic Science and Engineering, Huazhong University of Science and Technology, Wuhan 430074, China*

[2] *Britton Chance Center for Biomedical Photonics, Wuhan National Laboratory for Optoelectronic, Huazhong University of Science and Technology, Wuhan 430074, China*

[3] *Key Laboratory of Biomedical Photonics of Ministry of Education, Huazhong University of Science and Technology, Wuhan 430074, China*

[*] *Corresponding author: ydeng@mail.hust.edu.cn*

Received October 27, 2011; accepted January 10, 2012; posted online March 15, 2012

Combining photoacoustic (PA) imaging with laser speckle (LS) imaging (LSI) can simultaneously determine total hemoglobin concentration (HbT), hemoglobin oxygen saturation (SO2), and blood flow rates. Thus, the co-registration of PA and LS images is important in physiological studies and pathological diagnosis. This letter presents a co-registration algorithm combining mutual information with the maximum between-class variance segmentation method (Otsu method). The mutual information and Otsu method are used to provide the registration measure criterion and image feature recognition, respectively. The evaluation results show that the registration function possesses a single maximum peak and high smoothness across the global co-registration district, indicating a robust behavior. Moreover, this method has good registration accuracy, and the fusion result simultaneously visualizes the separate functional information of two kinds of images.

OCIS codes: 110.6150, 110.5120, 100.2000, 170.2655.
doi: 10.3788/COL201210.061101.

Photoacoustic (PA) imaging (PAI) is a rapidly emerging, noninvasive imaging method. It visualizes the structural and functional characteristics of biological tissues by ultrasonically detecting their optical absorption contrast of these tissues *in vivo*, breaking highly optical scattering limitations and achieving super-depth high-resolution optical imaging[1−3]. Thus, the method has been widely applied in monitoring angiogenesis, melanoma, hemoglobin oxygen saturation (SO2)[4], and total hemoglobin concentration (HbT)[1,2]. Laser speckle (LS) imaging (LSI), a no-scanning, noninvasive imaging tool, could achieve highly spatial (tens of microns) and temporal (millisecond) resolutions for imaging biological tissues *in vivo*[5,6]. The temporal and spatial statistics of speckle pattern intensity fluctuations contain the movement information of the object observed. Local velocity distributions should be measured properly by analyzing local speckle contrast variations[6]. Thus, LSI is always used for monitoring capillary blood flow rates in the skin and cerebral blood flow rates[6−8]. Combining PA and LS images could simultaneously provide HbT, SO2, and capillary blood flow information. The multimodality image co-registration technology is the foundation of fusion, which is significant for understanding the normal and pathophysiological conditions of neurovascular, metabolic, and hemodynamic interactions[9,10]. These multimodality co-registration methods can be classified as either extrinsic, intrinsic (including landmarks, segmentation- and mutual-information-based registration), or non-image-based registration methods[11,12]. The mutual information method does not need assumptions and limiting constraints for the image content. Thus, it is a very general and powerful criterion for multimodality image co-registration. However, mutual information is only sensitive to gray-level distribution and does not include spatial information. Therefore, it fails in some multimodality co-registration methods[13]. For example, the gray levels of the PA and LS images characterize different functional information rather than spatial information. However, both images possess high imaging resolutions and provide high imaging contrast between vascular and background tissues. Hence, the threshold segmentation methods for spatial feature recognition are feasible. This letter proposes a method that combines the maximum between-class variance segmentation (Otsu method) and mutual information methods. This method can be used to co-register PA and LS images.

The Otsu method for pixel-based global thresholding can be used to extract the salient structures of the images. It is a widely used automatic threshold selection method, which maximizes the separability of the resultant classes in gray levels to calculate the optimal threshold[14]. The pixels of a given image are represented in L gray levels. The number of i level pixels is N_i, and the probability distribution can be normalized by the gray-level histogram

$$P_i = \frac{N_i}{\sum_{i=0}^{L-1} N_i}, P_i \geqslant 0, \sum_{i=0}^{L-1} P_i = 1. \quad (1)$$

Then, a threshold at the kth level could dichotomize the original picture into two classes C_0 and C_1 (background

and object, respectively). C_0 denotes the pixels at levels [1,2, $\cdots$, k], and C_1 denotes the pixels at levels [k+1, k+2, $\cdots$, L]. Then, the probabilities of class occurrence and the class mean levels are denoted as

$$\omega_0(k) = \sum_{i=0}^{k} P_i,\ \omega_1(k) = \sum_{i=k+1}^{L-1} P_i, \tag{2}$$

$$\mu_0 = \sum_{i=0}^{k} \frac{iP_i}{\omega_0},\ \mu_1 = \sum_{k+1}^{L-1} \frac{iP_i}{\omega_1}, \tag{3}$$

and $\mu_{\mathrm{T}} = \sum_{i=0}^{L-1} iP_i$ is the total mean level of the original picture. The discriminant criteria are introduced to evaluate the class separability or the "goodness" of the threshold at level k, which is denoted as

$$\sigma_{\mathrm{B}}^2(k) = \omega_0(k)[\mu_0(k) - \mu_{\mathrm{T}}]^2 + \omega_1(k)[\mu_1(k) - \mu_{\mathrm{T}}]^2, \tag{4}$$

where $\sigma_{\mathrm{B}}^2(k)$ is the between-class variance, which is a function of threshold level k. The optimal threshold k^* would maximize $\sigma_{\mathrm{B}}^2(k)$. The optimization issue is to search a threshold k^* that maximizes the criterion functions, that is

$$\sigma_{\mathrm{B}}^2(k^*) = \max_{1<k<L} \sigma_{\mathrm{B}}^2(k). \tag{5}$$

Mutual information is used as a feature matching (measures) criterion[13], which measures the statistical dependence between two images A and B. It could be described by the following equations with entropy:

$$\begin{aligned} I(\mathrm{A},\mathrm{B}) &= H(\mathrm{A}) + H(\mathrm{B}) - H(\mathrm{A},\mathrm{B}) \\ &= H(\mathrm{A}) - H(\mathrm{A}|\mathrm{B}), \end{aligned} \tag{6}$$

where I(A,B) is the mutual information of images A and B; H(A) and H(B) denote the marginal entropy values of A and B, respectively, which could be computed by the probability distributions of the image intensities; H(A,B) denotes the joint entropy; H(A|B) denotes the conditional entropy of A given B. They are defined as

$$H(\mathrm{A}) = -\sum_{a} P_{\mathrm{A}}(a) \log_2 P_{\mathrm{A}}(a), \tag{7}$$

$$H(\mathrm{A},\mathrm{B}) = -\sum_{a,b} P_{\mathrm{AB}}(a,b) \log_2 P_{\mathrm{AB}}(a,b), \tag{8}$$

$$H(\mathrm{A}|\mathrm{B}) = -\sum_{a,b} P_{\mathrm{AB}}(a,b) \log_2 P_{\mathrm{A|B}}(a|b), \tag{9}$$

assuming that A is the reference image and B is the floating image. In the registration process, image A remains geometrically unchanged, whereas image B executes the affine transformation. According to Eqs. (5) and (7), H(A) remains invariable in the process, whereas H(A|B) varies as the affine transformation of image B. When the co-registration image pair is geometrically aligned, H(A|B) reduces to the minimum and the mutual information I(A,B) increases to its maximal value.

The Powell method is used as the optimization of the registration function, involving three dimensions of search space: the horizontal and vertical transformations and the rotation around the image center. Convergence, that is, three dimension optimizations, is achieved by repeatedly performing the Powell method in each search space dimension.

The LS and PA images are defined as the reference and floating images, respectively. The LS images are obtained by calculating the speckle contrast in the spatial domain after the LSI of the rat skull. The LSI resolution used in the experiments is 13 μm[15]. Meanwhile, the PA images are obtained using a reflection-mode PA microscope (PM) to scan the rat skull. The lateral resolution of the rat brain is 30 μm[16]. Before the registration process, the LS images are interpolated to match their image resolutions. Then, according to the imaging matrix sizes of the PA images, the quasi-identical field of view (FOV) is experientially extracted from the LS images, which seem to possess a broader FOV after interpolation. The extracted FOV is 1.6×2.8 (mm), and the imaging matrix size is 50×90. After the aforementioned operations, the LS and PA images for registration appear as shown in Figs. 1(a) and (b), respectively.

The salient features and vascular skeleton of the reference and floating images are extracted, as shown in Figs. 1(c) and (d). The geometrically aligned figures (Figs. 1(e) and (f)) can be obtained by computing the mutual information between the vascular skeleton image pairs and by optimizing the affine transformation parameters. The co-registration time for the aforementioned imaging size is about 2 s, which is acceptable in practice.

The performance of the method is evaluated according to three aspects: mutual information function behavior, registration accuracy, and fusion result analysis. The registration function behavior illustrates the robustness of the registration method. Figure 2 shows the co-registration function behavior in the rotation dimension. It is obtained by applying a continuous affine transformation in [−20°, 20°] to the well-registered vascular skeleton damage of the PM and by calculating the mutual information values of the range image pairs. The co-registration function in Fig. 2 appears maximal if the reference and transformed floating images are

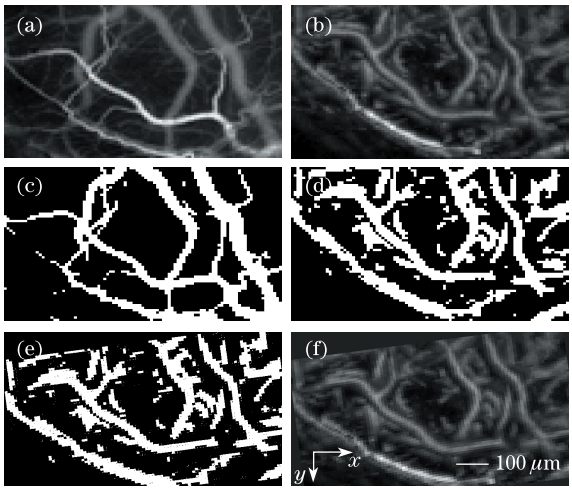

Fig. 1. Original (a) LS and (b) PM images, vascular skeleton features of the (c) LS and (d) PM images, (e) registered feature, and (f) original PM image.

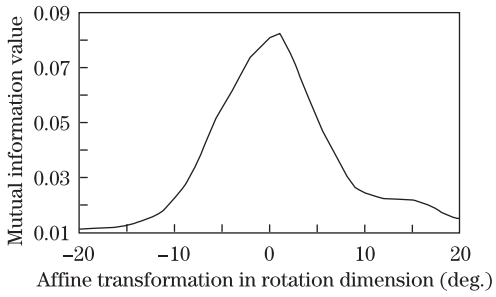

Fig. 2. Co-registration function of LSI and PAI.

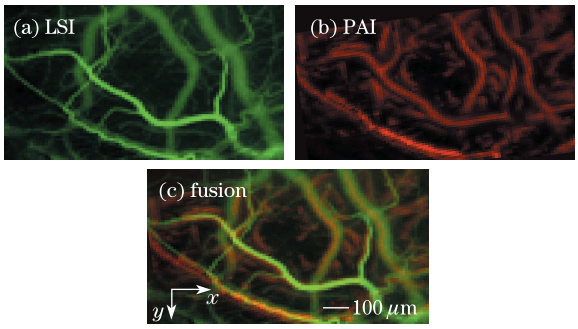

Fig. 3. (Color online) Fusion results of the co-registration method. Green and red pseudocolor (a) LS and (b) PA images, respectively, and (c) fused LS and PA images after the weighted average method.

geometrically aligned and the registration behavior varies smoothly across the global district. Both of these conditions indicate that the combination method is highly robust[17].

The co-registration accuracy is evaluated by comparing the registration results and affine transformation parameter setting. In 100 registration experiments, the parameters are uniformly and randomly distributed: The horizontal and vertical variables are randomly distributed in the [−15, 15] pixel district, and the rotation variables are randomly distribute in the [−10°, 10°] district. The co-registration accuracy is illustrated by the registration error between the registration results and the setting parameters

$$\Delta x = |x_{\rm r} - x_{\rm s}|,\ \Delta y = |y_{\rm r} - y_{\rm s}|,\ \Delta{\rm ang} = |{\rm ang}_{\rm r} - {\rm ang}_{\rm s}|, \quad (10)$$

where $x_{\rm s}$, $y_{\rm s}$, and ang$_{\rm s}$ are the three dimensions of the affine transformation setting in the experiments, respectively, whereas $x_{\rm r}$, $y_{\rm r}$, and ang$_{\rm r}$ are the three dimensions of the registration results of the proposed method in the experiments. The mean errors of the 100 registration experiments are $\overline{\Delta x}$=2.41 pixels, $\overline{\Delta y}$=3.27 pixels, and $\overline{\Delta{\rm ang}}$=0.35°. The spatial resolution of the images registered is 30 μm. Thus, the co-registration accuracy could be given as 72.1 μm, 98.1 μm, and 0.35° in the lateral, longitudinal, and rotating deviations.

In practical psychological studies or clinical treatments, subjective evaluation is important in multimodality image co-registration. The enhanced pseudocolor LS and PA images are shown in Figs. 3(a) and (b), respectively. The green values of the LS image correspond to the blood flow rates, whereas the red values of the PA image correspond to the optical absorption. Then, the registration images are fused using the weighted average method[18]. The fusion image is shown in Fig. 3(c), where the HbT, SO2, and blood flow rates are simultaneously indicated.

In conclusion, PAI and LSI visualize different functional information of the same biological tissues. Co-registration is important in simultaneously monitoring some physiological features, such as SO2, HbT, and capillary blood flow rates. Based on the characteristics of the PA and LS images, we propose a method that combines feature detection and mutual information measurement. The registration results indicate that the method possesses good co-registration function behavior, containing a single maximum and high smoothness across the global district. At the same time, the co-registration statistical results show the acceptable, but still to be improved, co-registration accuracy. Two dominating aspects limit the registration accuracy: PAI, the lower resolution imaging of the two methods, imposes a restriction, whereas the Otsu method only delineates the skeleton of the large vessels for registration, implying that high-resolution parts could not be employed. For substantial amount of intermediate and capillary vessels appearing in the future, a two-resolution scale via the pyramid model could be employed in the next step to optimize the high-resolution registration regionally along with the low-resolution registration[19].

This work was supported by the National Major Scientific Research Program of China (No. 2011CB910401), the Science Fund for Creative Research Group of China (No. 61121004), the National Natural Science Foundation of China (No. 61078072), and the Fundamental Research Funds for the Central Universities, Huazhong University of Science and Technology (No. 2010MS111).

References

1. S. Hu and L. V. Wang, J. Biomed. Opt. **15,** 011101 (2010).
2. H. F. Zhang, K. Maslov, G. Stoica, and L. V. Wang, Nat. Biotechnol. **24,** 848 (2006).
3. L. V. Wang, IEEE J. Sel. Top. Quantum Electron. **14,** 171 (2008).
4. K. Maslov, H. F. Zhang, S. Hu, and L. V. Wang, Opt. Lett. **33,** 929 (2008).
5. J. D. Briers, Opt. Applicata **XXXVII,** 139 (2007).
6. H. Cheng, Q. Luo, Q. Liu, H. Gong, and S. Zeng, Phys. Med. Biol. **49,** 1347 (2004).
7. J. D. Briers, G. Richards, and X. W. Xiao, J. Biomed. Opt. **4,** 164 (1999).
8. A. K. Dunn, H. Bolay, M. A. Moskowitz, and D. A. Boas, J. Cerebr. Blood F. Met. **21,** 195 (2001).
9. A. K. Dunn, A. Devor, H. Bolay, M. L. Andermann, M. A. Moskowitz, A. M. Dale, and D. A. Boas, Opt. Lett. **28,** 28 (2003).
10. A. Devor, A. K. Dunn, M. L. Andermann, I. Ulbert, D. A. Boas, and A. M. Dale, Neuron **39,** 353 (2003).
11. J. B. A. Maintz and M. A .Viergever, Med. Image Anal. **2,** 1 (1997).
12. B. Zitova and J. Flusser, Image Vision Comput. **21,** 977 (2003).
13. F. Maes, A. Collignon, D. Vandermeulen, G. Marchal,

and P. Suetens, IEEE Trans. Med. Imag. **16,** 187 (1997).
14. N. Otsu, IEEE Trans. Syst. Man. Cy. **9,** 62 (1979).
15. X. Yang, X. Cai, K. Maslov, L. Wang, and Q. Luo, Chin. Opt. Lett. **8,** 609 (2010).
16. J. Qiu, P. Li, W. Luo, J. Wang, H. Zhang, and Q. Luo, J. Biomed. Opt. **15,** 016003 (2010).
17. J. P. W. Pluim, J. B. A. Maintz, and M. A. Viergever, IEEE Trans. Med. Imag. **19**, 1 (2000).
18. C. Pohl and J. L. Van Genderen, Int. J. Remote Sensing **19,** 823 (1988).
19. P. Xu and D. Yao, Comput. Biol. Med. **37,** 320 (2007).